

# Enhanced Sensitivity of Two-Dimensional Bar-Codes Microfluidic Paper-Based Device ( $\mu$ PADs) By Gold Nanoparticles

Jingjing Liu<sup>1,2\*</sup>, Linyan Li<sup>1</sup>, Qian Huang<sup>1</sup>, Jiaqi Yang<sup>1</sup>, Fei Guo<sup>1</sup>, Xiao Li<sup>1</sup>, Zhe Liu<sup>1</sup> and Tengfei Wang<sup>1</sup>

<sup>1</sup>School of Information Technology, Suzhou Institute of Trade & Commerce, Suzhou, P. R. China

<sup>2</sup>Division of Nano Bionic Research, Suzhou Institute of Nano-Tech and Nano-Bionics, Chinese Academy of Sciences, Suzhou, P. R. China

**\*Corresponding author:** Jingjing Liu, School of Information Technology, Suzhou Institute of Trade & Commerce, Division of Nano Bionic Research, Suzhou Institute of Nano-Tech and Nano-Bionics, Chinese Academy of Sciences, Suzhou, P. R. China, E-mail: [jjliu2015@sinano.ac.cn](mailto:jjliu2015@sinano.ac.cn)

**Citation:** Jingjing Liu, Linyan Li, Qian Huang, Jiaqi Yang, Fei Guo, et al. (2020) Enhanced Sensitivity of Two-Dimensional Bar-Codes Microfluidic Paper-Based Device ( $\mu$ PADs) By Gold Nanoparticles. *J Nanosci Nanotechnol Appl* 4: 102

## Abstract

Microfluidic paper-based devices ( $\mu$ PADs) has been studied extensively for rapid detection. However, the sensitivity of the detection are sacrificed for the rapid detection, which might be promote by plasmonic gold nanoparticles. In this paper, we demonstrated the  $\mu$ PADs with Au nanoparticles integrated which could be used as a multi-metallic ion sensor for point-of-care testing. By combining the fast, accurate, convenient, and direct merits of a smartphone-based colorimetric readout with the designed  $\mu$ PADs device, we could obtain relevant information such as the type of ion and relative concentrations. We optimized the information area, outline geometry, and reduction rate of  $\mu$ PADs information areas. The metallic ion concentrations could be determined in the linear dynamic range of 1~20 mg L<sup>-1</sup> for Al<sup>3+</sup> and 2~20 mg L<sup>-1</sup> for Cr<sup>6+</sup> and Zn<sup>2+</sup>. The proposed  $\mu$ PADs sensor can achieve quantitative detection of metallic ion which was found to be highly sensitive for metallic ion detection against non-AuNPs. In addition, the prepared sensor was successfully applied to assay metallic ion in real environmental samples.

**Keywords:** Gold Nanoparticles; Paper-Based Devices; Multi-Metallic Ions Detection

## Introduction

Point of care testing (POC) has a unique analytical detection advantages, which is widely used in infectious diseases [1,2], food safety [3], environmental monitoring [4]. For the first time presented by Whitesides research group in 2007 [5], paper as a substrate to construct microfluidic paper-based devices ( $\mu$ PADs) has been studied extensively for rapid detection [6,7]. The fluid that driver by capillarity wick in two or three dimensions, which play a very important role in point of care (POC) diagnostic testing [8]. Colorimetric assay has experienced rapid development, which is expected to achieve each person's low cost for POC diagnosis testing [9]. Towards accurate quantification, several groups have tried various optical detector scanning<sup>10</sup>, cameras [11], smart phones [12] to analyse colorimetric detection. Although colorimetry can achieve quantitative analysis [13], this visual detection rely on the colour intensity or brightness on paper, which often bring a lot of uncertainty [14].

As the increasing of using smartphone based biosensor, potentially, the smartphone based detection technology provides an ideal platform for the rapid detection technology [15-17]. Meanwhile, the two-dimensional (2D) bar code is prevalent used in daily life in terms of payment, browsing the web and so on. Thus, in this approach, we utilized the complex motif of two-dimensional code to construct the hydrophobic and hydrophilic barriers, which can be scanned by smart phones. This new colorimetric analysis is kind of method using distance-based detection in paper [18]. In the distance-based detection principle, the analyte reacts with color agent and grows along the flowing stream line until all the analyte is depleted. Distance-based measurement for paper analytical devices has been successfully achieved in the horizontal direction of the quantitative analysis of heavy metals and glucose [15,19]. These distance detection methods have limitation in practical applications. First, in the horizontal direction distance method detection, color agent and analyte need more order of magnitude for a longer period of time to complete detection and the volatile liquid in the process will be faced. Second, more color products will be gathered in the fluid terminal that makes the distance detection in directly by naked eye observation appear larger error and difficult to identify.

There is growing explosion in the broadband light absorbers because of their importance in various application, such as surface-enhanced spectroscopy, solar energy conversion, photothermal therapy, and fabrication of novel optoelectronic devices. To improve the detection sensitivity, our new designed 2D bar code PADs with gold nanoparticles integrated which have the advantages to minimize the error which caused by the long distance on the horizontal channel. We proposed a convenience detection method that the result of a colorimetric detection could be obtained by scanning a 2D barcode via a smartphone. In this study, we also optimized the surface area, geometry, and reduction rate of  $\mu$ PADs information areas for the real-time, effective, and accurate detection of metallic ions ( $\text{Al}^{3+}$ ,  $\text{Cr}^{6+}$ , and  $\text{Zn}^{2+}$ ).

## Experimental

All chemicals were used without any further purification and ultrapure water purified with a Mill-Q system (18.2 M $\Omega$  cm) from Merck Millipore (Darmstadt, Germany). Ammonium aluminium sulfate dodecahydrate, zinc nitrate hexahydrate, chrome azurol S, zincon disodium salt, 1,5-diphenylcarbazine (DPC, acetone, mercury(II) sulfate, iron (III) chloride anhydrous, copper (II) sulfate pentahydrate, sodium acetate, acetic acid glacial and manganese sulfate anhydrous were purchased from Sinopharm Chemical Reagent Company (Shanghai, China). Potassium dichromate was purchased from Guangzhou Jinhua Chemical Reagent Company (Guangzhou, China). Lead nitrate and magnesium sulfate anhydrous were purchased from Aladdin (Shanghai, China). Nickel (II) nitrate was purchased from Enox (Jiangsu, China). Qualitative-grade filter paper was purchased from the Xinhua paper company (Hangzhou, China). Hydrophobic wax was used as barrier for all detection types. Adobe illustrator software (Creative Cloud 2014) was used for the design of the patterns. The  $\mu$ PADs were patterned by a commercially available wax printer (FUJIXEROX Phaser 8560DN).

The overall design concept and operation flow chart is shown in Figure 1. The fabrication procedure involves using Adobe illustrator to design the information area and hydrophilic sample reservoirs, each analytical device were sized as 20 x 20 mm<sup>2</sup>. Then, the hydrophilic-hydrophobic contrast of patterns were printed on the appropriate sized filter paper using a commercial wax printer. The multiple information of the two-dimensional barcode that is composed of hydrophobic wax and hydrophilic reagents' reservoirs. Three white zone (Figure 1) which is the hydrophilic zone set as the testing area at the centred accommodate sample addition. We used commercial  $\mu$ PADs software to scan and the information showed in the phone screen (Figure S1).

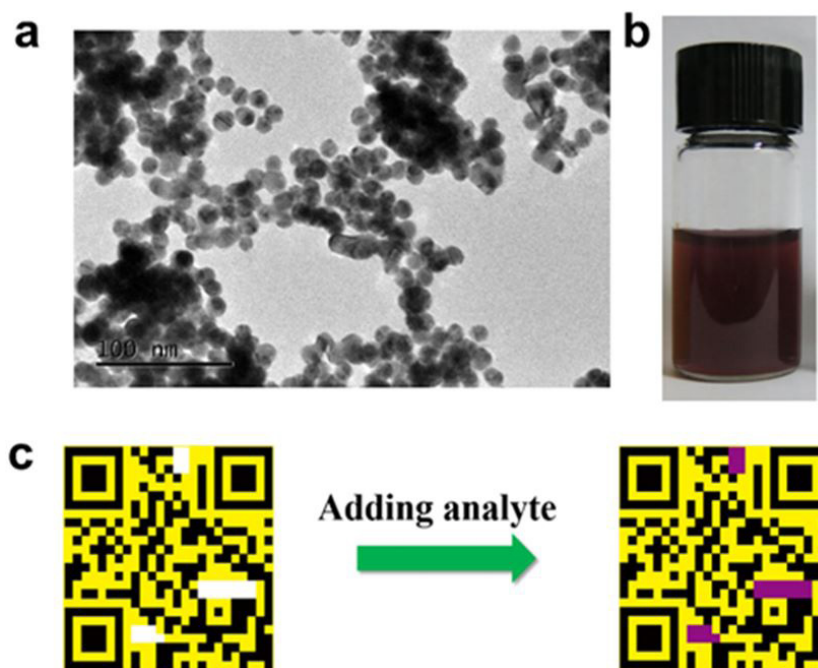


**Figure 1:** Operational concept of the two-dimensional code assay. Wax printing is simple, inexpensive and fast to fabricate the paper analytical devices. (a) TEM image of gold nanospheres with 15nm, the scale bar is 100nm; (b) The digital photo is a suspension of Au nanoparticles, the scale bar is 2cm (c) Schematic diagram and process flow of the  $\mu$ PADs paper-based device

## Results and Discussion

As shown in Figure 2, we provided six separated  $\mu$ PADs with different amount of Au nanoparticles (AuNPs) suspension dropped on the three rectangle reservoirs, the capillary action allowed the analyte to migrate quickly in the formed microchannel. The amount of the au nanoparticles are measured with weight percent of the suspension from L0 to L5. Finally, all the  $\mu$ PADs were separated sequentially for easy recognition which were scanned by using a smartphone. Compared to  $\mu$ PADs with non-AuNPs of L6, the sensitivity of the metal ion detection could be found by the intensity of the colorimetric reactions.

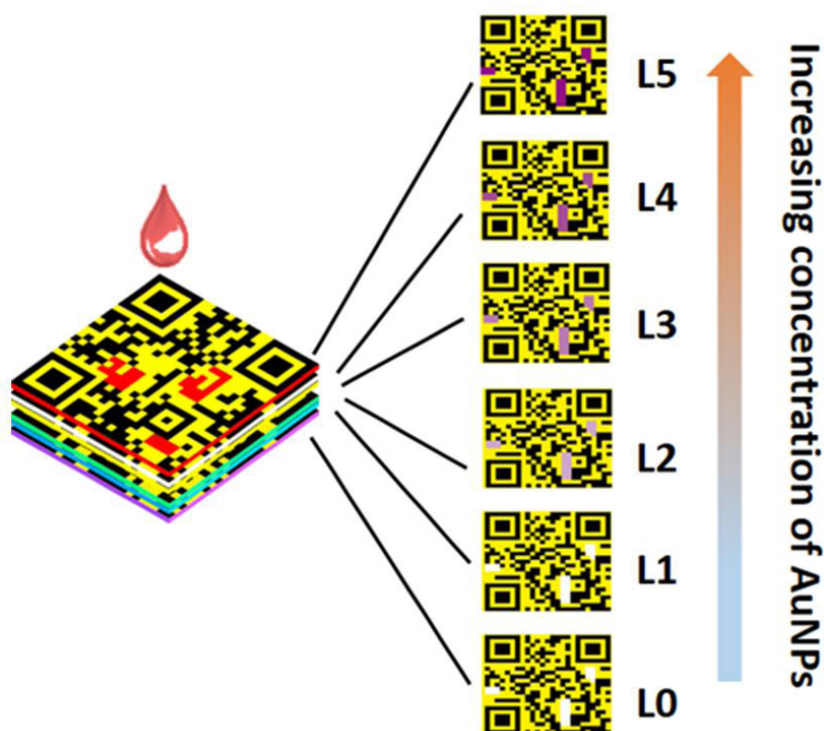


**Figure 2:** Six separated  $\mu$ PADs device. The separated six layers were denoted as L0, L1, L2, L3, L4, L5 (L5=1.0%, L4=0.6%, L3=0.5%, L2=0.2%, L1=0.1%, L0=0). The  $\mu$ PADs for the quantitative analysis was scanned by a smartphone

The recognition of  $\mu$ PADs in balance with the size of the information area needs to consider. It is shown in Table S1 that the percentage of the information area with gold nanoparticles compared to the total surface of the  $\mu$ PADs (%). We summarized the recognition capability of the smartphone depending on the different dimensions of the  $\mu$ PADs. To rapidly identify the  $\mu$ PADs information resulting from colorimetric reactions, the identification process was as follows. First, the  $\mu$ PADs was erased by increasing information area ratio ( $> 5.3\%$ , information area of the total surface of the  $\mu$ PADs as shown in Table S1). Second, the hydrophilic blank area containing the colorimetric reagents and the analyses reacted in the reaction region and the resulting products gradually covered the information area and the  $\mu$ PADs could be recognized by the smartphone. Finally, the sensitivity of the metal ions could be enhanced by the amount of AuNPs which could be recognized by the smartphone.

Wax printing appeared to be a simple and inexpensive method for the fabrication of  $\mu$ PADs [19]. The process involves the penetration of the wax pattern into the paper sheet by heat to form the hydrophilic and hydrophobic areas of the PADs. The heating step could lead to the shrinkage of the  $\mu$ PADs and could impede the recognition by the smartphone. In order to evaluate the influence of the heating step, we compared the reduction rate of  $\mu$ PADs information areas presenting an outline geometry of  $20 \times 20 \text{ mm}^2$  and prepared with and without heating. Wax spread inside the porous filter paper due to the capillary action characterized by the Washburn's equation (Eq. 1) [20]:

with  $t$  as the heating time;  $\eta$  as the viscosity of the liquid;  $\gamma$  as the surface tension;  $L$  as the flow distance, and  $D$  as the average pore diameter of the porous material.

$$L = \sqrt{\frac{\gamma D t}{4\eta}} \quad (1)$$

The results are depicted in the graphic shown in Figure 3. The average reduction rate of  $\mu$ PADs information areas was 47.9% and the relative standard deviation value (RSD) for all measurements ( $n=5$  measures for each different  $\mu$ PADs information area) was 9.3%. When the information area was too small, the bar-code information could not be recognized because the hydrophilic region was blocked by the melted wax.

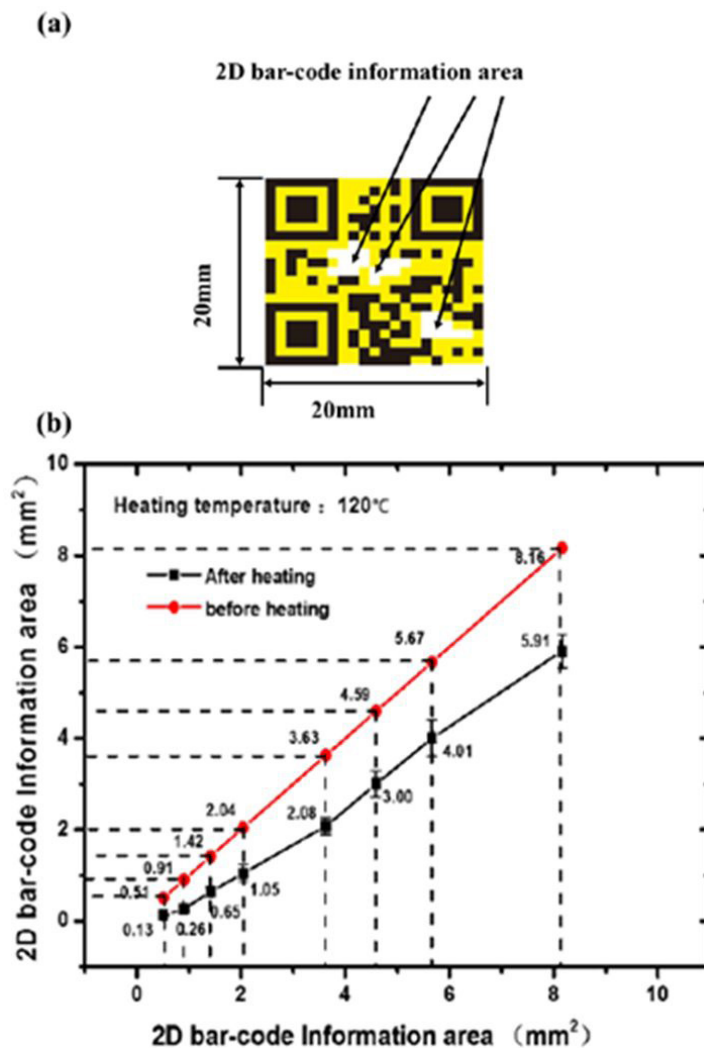


Figure 3: (a) μPADs information area with an outline geometry of 20 x 20 mm<sup>2</sup>. (b) The relation between the information area without and with heating process. The average reduction rate of μPADs information areas was 47.9% (n=5)

To clarify the sensitive capability of the μPADs, Figure 4 gives the resonances intensity various among different media or solution for L6 of μPADs. It is interesting that the variation of the resonances for the peak is tending to approach as the value increasing of different metallic ion solution. To further investigate the μPADs sensing capabilities of non-AuNPs and with AuNPs, the solution with different concentration was chosen and injected into 2D-bar codes based microfluidic channel (Table S2, ESI).

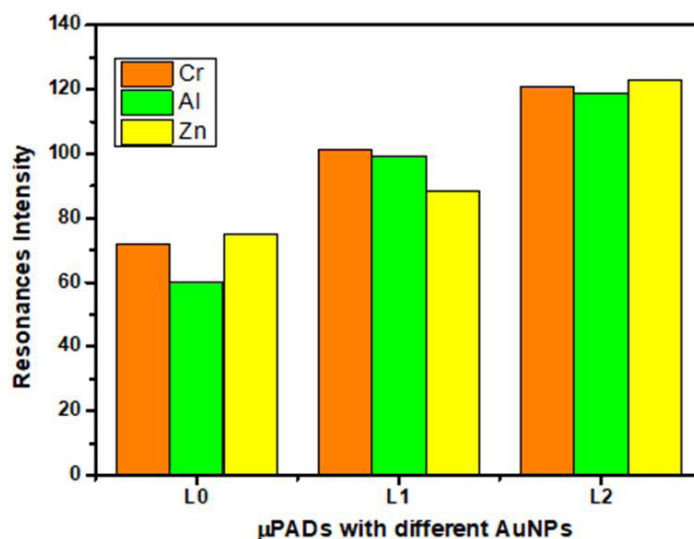
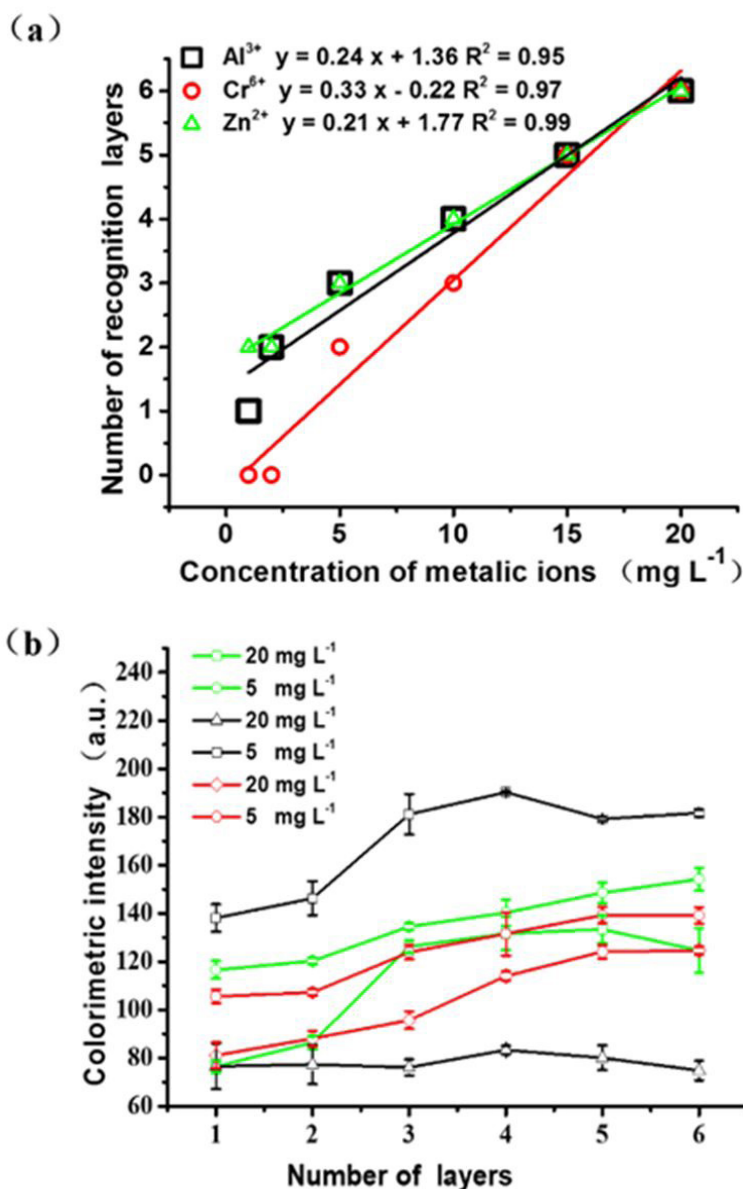


Figure 4: The resonant intensity various among different media or solution for Peak of μPADs

In order to evaluate the ability of the  $\mu$ PADs to detect metal ions quantitatively, we used a distance-based detection in the vertical direction [21]. As the distance-based detection presented a nonlinear fluid velocity-dependent, the colorimetric products responded non-linearly to the variation of distance in the vertical direction [22,23]. We developed a specific layer deposition method for Figure 4. The resonant intensity varies among different media or solution for Peak of  $\mu$ PADs dropping the colorimetric reagents on the paper surface to counter this non-linear response. Once the information area was completely dried, a single aliquot of the analyte was dropped on the hydrophilic information area of the first layer for the complete analysis of the sample. The colorimetric reagent reacted with the metallic ions of the sample to form colorimetric products, which were also on the paper surface of the 2D-bar codes. The concentration of the colorimetric products distributed continuously along the top to the bottom layers via micro channels.

The colorimetric reagent accumulation gradually became less pronounced from top to bottom as the number of total layers increased. The results are depicted in Figure S2 and the relative standard deviation (RSD) for all measurements ( $n=5$  measures for each different stacked layers) was of 5.0%. To maximize the detection limit, we considered the highest number of 2D-bar codes stacked layers available. The flow rate inside the microchannel would be close to zero (when the number of layers is greater than 8) and the colorimetric products would stop being generated according to the Lucas Washburn theory. Nevertheless, the recognition layers with colorimetric reagents could be enhanced if the colorimetric reagent dosage and sample rate increased. However, exceeding a certain threshold, the colorimetric reagents would destroy the hydrophilic  $\mu$ PADs information area. The results indicated that the minimum path length (ca. 900  $\mu$ m) to be travelled by the fluid inside the device corresponded to the stacking of six layers. Therefore, the subsequent experiments were performed on 6-layers 2D-bar codes.



**Figure 5:** The recognition ranges of the 6 layer-device were 1 - 20 mg L<sup>-1</sup>, 2-20 mg L<sup>-1</sup>, 2-20 mg L<sup>-1</sup> for Al<sup>3+</sup>, Cr<sup>6+</sup> and Zn<sup>2+</sup> metallic ions, respectively. (b) The colorimetric intensities were used for the detection of Al<sup>3+</sup>, Cr<sup>6+</sup> and Zn<sup>2+</sup> metallic ions and the concentrations were 5, 5, and 20 mg L<sup>-1</sup>, respectively

In Figure 5a,  $\mu$ PADs devices were tested using the same analyte range ( $1\sim 20\text{ mg L}^{-1}$ ) for all three respective metal ions ( $\text{Al}^{3+}$ ,  $\text{Cr}^{6+}$ , and  $\text{Zn}^{2+}$ ). The experimental results indicated that the concentration of metallic ions could be quantified by counting the number of the layers recognized by the smartphone. The recognition linear dynamic range of the  $\text{Al}^{3+}$  metallic ions was  $1\sim 20\text{ mg L}^{-1}$ , while the one of the  $\text{Cr}^{6+}$  and  $\text{Zn}^{2+}$  metallic ions were  $2\sim 20\text{ mg L}^{-1}$ . The limits of detection of  $\text{Al}^{3+}$ ,  $\text{Cr}^{6+}$ , and  $\text{Zn}^{2+}$  were 1, 2, and  $2\text{ mg L}^{-1}$ , respectively. These values are similar to the ones referred in the World Health Organization (WHO) guidelines [24,25]. Overall, the data clearly showed that the  $\mu$ PADs detection of the metallic ions was possible with a smartphone (Figure 5a) without having to use a complex image analysis step for quantification. This proof of concept opens new avenues for the use of  $\mu$ PADs paper-based devices in many fields such as the direct in-field detection of metallic ions by avoiding the need for sophisticated and expensive instrumentation located in a central laboratory that is commonly required for further quantitative analysis [26,27].

To demonstrate the reliability of the detection, we determined the relation between the colorimetric intensity and the recognition rate as summarized in Figure 5b. As the colorimetric reagents and metal ions reacted, colored products were formed in the hydrophilic information area. Due to the different recognition rates of each metallic ions, appropriate concentrations had to be chosen in order to analyze the colorimetric intensity of the sample. We decided to use a maximum concentration of  $20\text{ mg L}^{-1}$  and a minimum concentration of  $5\text{ mg L}^{-1}$  for the  $\text{Al}^{3+}$ ,  $\text{Cr}^{6+}$  and  $\text{Zn}^{2+}$  metallic ions to evaluate the number of layers that could be recognized by a smartphone (the RSD were 4.3%, 6.8%, and 3.2%, respectively,  $n=3$ ). For the same metallic ion concentration, the colorimetric intensity increased together with the number of layers. And for the same number of layers in  $\mu$ PADs devices, the colorimetric intensity increased as the metallic ion concentration increased. As mentioned above, the concentration of the colorimetric products could gradually decreased from the top to the bottom layers, reducing the number of layers that could be recognized by the smartphone. At a metallic ion concentration of  $5\text{ mg L}^{-1}$  and under optimal colorimetric intensity and recognition condition of the  $\mu$ PADs in each layer, the measurement of the colorimetric intensity was above 140 ( $\text{Al}^{3+}$ ), 150 ( $\text{Cr}^{6+}$ ), and 140 ( $\text{Zn}^{2+}$ ), and the number of recognition layers were 4, 2, and 3, respectively. Paper based  $\mu$ PADs detection of  $\text{Al}^{3+}$ ,  $\text{Cr}^{6+}$ , and  $\text{Zn}^{2+}$  barely interfered by other ions, which also present in Figure S3.

## Conclusion

In summary, we designed and fabricated  $\mu$ PADs integrated with gold nanoparticles for multi-metallic ions real-time detection. We are able to simultaneously quantify the concentrations of three different metallic ions with high accuracy, and the limits of detection of  $\text{Al}^{3+}$ ,  $\text{Cr}^{6+}$ , and  $\text{Zn}^{2+}$  were 1, 2, and  $2\text{ mg L}^{-1}$ , respectively. We demonstrated a rapid method for the detection of metallic ions without the use of additional device, apart from the  $\mu$ PADs and a smartphone. The high portability, applicability, and cost-effectiveness of the  $\mu$ PADs detection approach would overcome the time and space limitations required in real-time diagnostic tests for environmental monitoring, food safety, and other fields.

## Acknowledgements

This research was supported by the Project of School of Information Technology (No. 701K502). Natural Science Foundation of Jiangsu Province (No. BK20190398) and the National Natural Science Foundation of China (No. 51802208).

## Electronic Supplementary Information (ESI)

## References

1. Wool GD (2019) Benefits and Pitfalls of Point-of-Care Coagulation Testing for Anticoagulation Management: An ACLPS Critical Review. *Am J Clin Pathol* 151: 1-17.
2. Chen H, Liu K, Li Z, Wang P (2019) Point of care testing for infectious diseases. *Clin Chim Acta* 493: 138-47.
3. Wu MYC, Hsu MY, Chen SJ, Hwang DK, Yen TH, et al. (2017) Point-of-care detection devices for food safety monitoring: Proactive disease prevention. *Trends Biotechnol* 35: 288-300.
4. Lewis GG, DiTucci MJ, Phillips ST (2012) Quantifying Analytes in Paper-Based Microfluidic Devices Without Using External Electronic Readers. *Angew Chem Int Ed* 51: 12707-10.
5. Martinez AW, Phillips ST, Butte MJ, Whitesides GM (2007) Patterned paper as a platform for inexpensive, low-volume, portable bioassays. *Angew Chem Int Ed Engl* 46: 1318-20.
6. Sackmann EK, Fulton AL, Beebe DJ (2014) The present and future role of microfluidics in biomedical research. *Nature* 507: 181-9.
7. Ota R, Yamada K, Suzuki K, Citterio D (2018) Quantitative evaluation of analyte transport on microfluidic paper based analytical devices ( $\mu$ PADs). *Analyst* 143: 643-53.
8. Gantelius J, Bass T, Sjöberg R, Nilsson P, Andersson-Svahn H (2011) A Lateral Flow Protein Microarray for Rapid and Sensitive Antibody Assays. *Int J Mol Sci* 12: 7748-59.
9. Rattanarat P, Dungchai W, Cate D, Volckens J, Chailapakul O, et al. (2014) Multilayer paper-based device for colorimetric and electrochemical quantification of metals. *Anal Chem* 86: 3555-62.
10. Weng CH, Chen MY, Shen CH, Yang RJ (2014) Colored wax-printed timers for two-dimensional and three-dimensional assays on paper-based devices. *Biomicrofluidics* 8: 066502.
11. Maxwell EJ, Mazzeo A,D, Whitesides GM (2013) Paper-based electroanalytical devices for accessible diagnostic testing. *MRS Bulletin* 38: 309-14.
12. Hong JI, Chang BY (2014) Development of the smartphone-based colorimetry for multi-analyte sensing arrays *Lab Chip* 14: 1725-32.
13. Khoshbin Z, Housaindokht MR, Izadyar M, Verdian A, Bozorgmehr MR (2019) A simple paper-based aptasensor for ultrasensitive detection of lead (II) ion. *Analytica Chimica Acta* 1071: 70-7.
14. Lewis GG, DiTucci MJ, Baker MS, Phillips ST (2012) High throughput method for prototyping three-dimensional, paper-based microfluidic devices. *Lab Chip* 12: 2630-3.

15. Cate DM, Dungchai W, Cunningham JC, Volckens J, Henry CS (2013) Simple, distance-based measurement for paper analytical devices. *Lab on a Chip* 13: 2397-404.
16. Liu X, Mwangi M, Li X, O'Brien M, Whitesides GM (2011) Paper-based piezoresistive MEMS sensors. *Lab Chip* 11: 2189-96.
17. Casto LD, Schuster JA, Neice CD, Baker CA (2018) Characterization of low adsorption filter membranes for electrophoresis and electrokinetic sample manipulations in microfluidic paper-based analytical devices. *Analytical Methods* 10: 3616-23.
18. Zhu H, Isikman SO, Mudanyali O, Greenbaum A, Ozcan A (2013) Optical imaging techniques for point-of-care diagnostics. *Lab Chip* 13: 51-67.
19. Carrilho E, Martinez AW, Whitesides GM (2009) Understanding Wax Printing: A Simple Micropatterning Process for Paper-Based Microfluidics. *Anal Chem* 81: 7091-5.
20. Fung KK, Chan CP, Renneberg R (2009) Development of enzyme-based bar code-style lateral-flow assay for hydrogen peroxide determination. *Anal Chim Acta* 634: 89-95.
21. Nie Y, Zhang X, Zhang Q, Liang Z, Ma Q, et al. (2020) A novel high efficient electrochemiluminescence sensor based on reductive Cu(I) particles catalyzed Zn-doped MoS<sub>2</sub> QDs for HPV 16 DNA determination. *Biosensors and Bioelectronics* 160: 112217.
22. Tsai TT, Shen SW, Cheng CM, Chen CF (2013) Paper-based tuberculosis diagnostic devices with colorimetric gold nanoparticles. *Sci Technol Adv Mater* 14: 044404.
23. Chen Y, Chu W, Liu W, Guo X (2018) *Sensors and Actuators B: Chemical* 260: 452-9.
24. Yang M, Liu Y, Jiang X (2019) Barcoded point-of-care bioassays. *Chem Soc Rev* 48: 850-84.
25. Yin X, Liang L, Zhao P, Lan F, Zhang L, et al. (2018) *J Mater Chem B* 6: 5795-801.
26. Perera ATK, Phan DT, Pudasaini S, Liu Y, Yang C (2020) Enhanced sample pre-concentration by ion concentration polarization on a paraffin coated converging microfluidic paper based analytical platform. *Biomicrofluidics* 14: 014103.
27. Ng JS, Hashimoto M (2020) *RSC Advances* 10: 29797-807.